THE EFFECTS OF RADIATION ON THE
OPTICAL CHARACTERISTICS OF
(SiO_2 + ZrO_2 ON Si SUBSTRATE) MIRRORS

by

Mark Anthony Ferrel

B.S., Emporia State University, 1983
B.S., Kansas State University, 1984

A MASTER'S THESIS

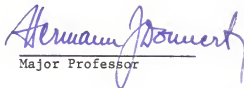submitted in partial fulfillment of the
requirements for the degree

MASTER OF SCIENCE

Department of Nuclear Engineering

KANSAS STATE UNIVERSITY
Manhattan, Kansas

1986

Approved by:

Major Professor

Table of Contents

LIST OF FIGURES

iii

LIST OF TABLES

1. INTRODUCTION

Determining nuclear-radiation effects on the optical subsystems of laser components, such as mirrors and windows, has recently become a matter of vital interest to those working on Strategic Defense Initiative (SDI) projects. This knowledge is very important for the design of anti-missile defense systems using lasers. Understanding the response kinetics along with formulating theoretical models will be essential to harden these systems and reduce their vulnerability. A major source of potentially damaging radiation to any SDI system is the nuclear reactor which may be used to pump the laser. (At this time nuclear reactor pumped laser systems are receiving a lot of attention as the method to deliver the energy needed to destroy a hostile projectile.)[1] If the optical components of the laser are susceptible to radiation generated by the reactor, the resulting induced absorption could cause the system to fail.

Because SDI includes space based systems, the effects of the natural radiation (electrons) present in space must also be considered a potential threat to the optical components.[2]

Radiation induced absorption by optical components in a Inertial Confinement Fusion (ICF) System is also undesirable. Because of the large amount of energy required at the fuel pellet site, any radiation absorbed by the optical components could be fatal to the ICF system.

Based on the common knowledge of solid-state physics, energy deposition from absorption of nuclear radiation, the microstructure of the crystal lattice, and the distribution of the electrons and holes in

1

quantum-mechanically available energy states, potential damage mechanisms can be predicted. Inevitable impurities and dislocation defects must also be accounted for when predicting potential damage mechanisms. Such defects impact a variety of physical properties to the solid material, such as electrical conductivity and optical absorbance. Thus, the question is not whether effects will actually occur, the question is, what is the magnitude of the effects and associated significance for either military systems design or inertial confinement fusion systems design.

Except for very preliminary efforts by this author, Hermann Donnert,[3] Gary Scronce,[4] and Kevin Stroh[5] at Frank J. Seiler Research Laboratory (FJSRL), virtually no research to explore this problem has been reported.[6] Although interesting, published observations of nuclear-irradiation effects on the performance of fiber optics[7] are of limited value in addressing the laser-component problem because solid-state behavior is little understood and current theories often do not apply.

Because of the extensive damage that could result from the failure of a SDI system, understanding the damage mechanism of the system is extremely important. Once the damage mechanisms are understood, mathematical models can be produced that will accurately predict damage to a system in a given environment. From these models, the best safeguards can be chosen to increase the system's reliable lifetime.

1.1 Objectives

The primary purpose of this research is to develop a basic understanding of how iodine laser mirror properties are affected by irradiation. In order to meet this goal the following objectives were identified:

a) determine the 50% iodine laser damage threshold (defined in Section 2.1.3) of the iodine laser mirrors,

b) mathematically model the iodine laser damage data,

c) develop a relationship between maximum mirror reflectivity and mirror vulnerability to iodine laser damage,

d) determine whether neutron irradiation will have an effect on the reflectivity of the mirrors, and

e) determine whether gamma irradiation will have an effect on the reflectivity of the mirrors.

Knowledge gained from the research about how and why these iodine laser mirrors are damaged will begin to form a basis for testing other laser components. The damage information will also provide a method for comparing the effectiveness of laser mirrors and components.

2. THEORY

2.1. DEFINITION OF TERMS

2.1.1. Fluence (J/m^2)

Fluence is the amount of laser energy in Joules that is incident on a surface area measured in meters squared. Fluence is an important parameter when performing laser damage tests on material: it is a measure of how dense the laser beam "photons" are. The procedure used to measure fluence will be discussed in section 4.2.

2.1.2. Iodine Laser Damage

For discussion in this paper, iodine laser damage will be defined as any "detectable" damage produced by an iodine laser shot (λ = 1.315 μm) at a given fluence (J/m^2) to the layered ($SiO_2 + ZrO_2$ on Si Substrate) dielectric coatings of the iodine laser mirrors. "Detectable damage" is damage that can be detected by the human eye under a microscope at a power of 200χ. Manufactured defects (defects present before experimentation began) were noted prior to testing. Except the as noted manufactured defects, defects are assumed to be homogeneous throughout the 20 mirrors since they all are from the same batch.

Damage produced by the iodine laser pulses were easily distinguished from manufactured defects by shape and depth. Damage caused by an iodine laser pulse generally have a very one-dimensional circular pattern. The circular pattern had rings within each other progressively getting smaller, resembling a rifle target. Manufactured defects on the other hand, had no distinct pattern. Manufactured

4

defects also show much more two-dimensionality, much more depth. These differences can be seen in Appendix A.

2.1.3. Laser Damage Threshold

The laser damage threshold is the iodine laser fluence (J/m^2) that would cause detectable damage on the tested iodine laser mirror 50 percent of the time. The laser damage threshold provides a common reference point for comparing the response of different materials and/or different manufacturing techniques to each other. This is the definition generally reported in literature.[8] The laser damage threshold is easily calculated once a mathematical model has been fit to laser damage data.

3. IODINE LASER MIRRORS

3.1 MANUFACTURING

The Rocketdyne Division of Rockwell International was contracted to manufacture the twenty 1-inch silicon mirrors to be tested for radiation damage. The mirrors were produced at Kirtland Air Force Base in New Mexico under the direct supervision of Gloria Petty (Job Number 40309-1, Subtask Number 03010).

3.1.1. Pre-Coating Preparation

The 1-inch diameter silicon wafers were first flushed with methanol to remove surface dirt. The edges were then cleaned with "Scotchbrite". The Si wafers were then given a one-minute cycle in the smooth ultrasonic Trichloroethane. They were then cleaned with methanol and cheesecloth followed by drying with "Genesolve DS" solvent. At this point it was noted that "there were small, evenly spaced pits or something that would not clean off."

Transmission measurements were then performed on both sides of each Si wafer. The side with the highest transmission was marked with a small piece of scotch tape. The side with the lowest transmission, was then coated as described below.

3.1.2. Coating Procedure

Alternating coatings of Zirconium dioxide and Silicon dioxide were deposited on the 1-inch diameter silicon wafers. Each ZrO_2 layer was 178 nm thick and had a refractive index of 1.85 while the SiO_2 layers were 228 nm thick and had a refractive index of 1.44.

With the Si wafer temperature at 150°C the first ZrO_2 layer was deposited at (0.5 ± 0.1) nm/sec using E-beam deposition. After one hour (soak time) elapsed, an SiO_2 layer was deposited at (1.0 ± 0.3) nm/sec using E-beam deposition. After one hour had elapsed the second layer of ZrO_2 was applied as before. This ZrO_2 then SiO_2 coating procedure was continued until 23 dielectric coatings had been applied. The Mirror Coating Information Sheet, Table (1) gives a more complete description of the dielectric coating process.

3.2 REFLECTIVITY MEASUREMENTS

Before the mirrors were damage tested, their reflectivity from 900 nm to 1500 nm was measured. The reflectivity measurement was spectral because any phase shift caused by radiation damage was expected to show up at a wavelength where the mirrors are less efficient.

The reflectivity measurements were performed at the Air Force Weapon Laboratory (AFWL) at Kirtland Air Force Base in New Mexico. Using a total integrated scatter spectrometer designed and custom-built at AFWL and supervised by Dr. Donnert of KSU, Gloria Perry measured the mirrors' reflectivity. Reflectivity spectrum of several mirrors can be seen in Appendix D. The spectrometer measured reflectivity squared using double bounce. The output was a continuous curve printed on graph paper. The squared reflectivity was read from each graph at increments of 4 nm. At peaks and valleys increments of 2 nm were used. If, as in many cases, the reflectivity spectrum was measured more than once for a single mirror, the reflectivity at each wavelength was averaged. The reflectivity vs. wavelength was then plotted for each mirror. When more

TABLE 1. Mirror Coating Information Sheet

Subtask #03010
Job #40309-1
Completion Date: May 1, 1984

Method: Optical Mochromator set at half
wavelength and shoot half waves

MONITOR DATA

Dial Setting	310
Slit Width	100 μm
Inc. Angle	4°
Monitor Material	Al_2O_3
Piece Size	1 inch

HEATER DATA

Substrate Temperature	150°C
Monitor Temperature	150°C
Time to heat to Temperature	3 hours
Soak Time	1 hour

Evaporants	ZrO_2	SiO_2
Vendor	Cerac	Cerac
Method of Evaporation	E-Gun	E-Gun
Deposition Rate	0.5 ± 0.1 nm/s	1.0 ± 0.3 nm/s
Initial Pressure	3.1 (-6)	3.1 (-6)
Deposition Pressure	3.0(-5) (O_2)	3.0(-5) (O_2)
Power Setting	6kV => 200-250 ma	6kV => 120 ma
	(IND)	(IND)

The process above produced mirrors who's maximum reflectivity was at
1.315 μm.

8

than one spectrum was used to calculate the reflectivity for a mirror, it will be stated along with the orientation of each measurement.

4. DESCRIPTION OF METHODOLOGY

4.1 Description of Equipment

The Iodine Atomic Laser, which was borrowed from Sandia Laboratories in New Mexico by the Air Force Academy to do several iodine laser damage tests, was manufactured "in house" at the Sandia National Laboratory. One of the laser damage tests is described in this paper.

A Schematic diagram of the experimental setup is shown in Figure 1 and the equipment used is listed in Table 2.

The iodine laser used I_6 as the lasing medium. The I_6 was stored as a liquid, converted to a gas when needed, and pumped into the laser cell (cavity) to a given pressure measured in Torr. A bank of capacitors was used to provide the voltage for lasing. The laser was a one shot-at-a-time procedure, described later. The laser output fluence (J/m^2) was controlled by either adjusting the I_6 pressure in the cell or by changing the capacitor voltage.

When the desired fluence could not be produced by changing the I_6 pressure or the capacitor voltage, neutral density filters were placed just in front of the iodine laser; these filters acted as an external control of laser fluence.

After passing through the neutral density filter, the beam was reflected 90° by mirror A and traveled to mirror B. At mirror B five percent of the beam was passed through the mirror to Gentec #3a.

Gentec #3a, a photodiode system, measured the energy (J) output of the laser. To increase the accuracy of the Gentec output (an analog output) an analog- to-digital converter (manufactured by Heathkit) was used.

10

Figure 1. Schematic Diagram of Iodine Laser Damage Test Equipment Setup
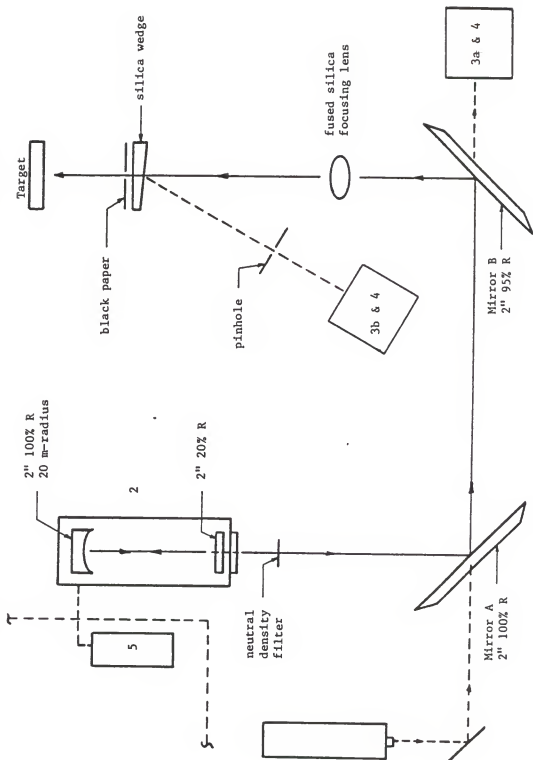
TABLE 2. Iodine Laser Image Test Equipment List

1) Helium-Neon Laser 155, 95 mW combined with He-Ne Laser Exciter
    Model 102-1, 4 mW both made by Spectra Physics.

2) Sandia Iodine Atomic Laser #T763607913 from Sandia
    Laboratories

    The Iodine Laser had the following support equipment:

    a) Lambda Regulated Power Supply Model LM D28R
        Serial #099240, Lambda Electronics Corporation.

    b) 2 Digital Pressure Indicators
        Torris A
        Spectra Systems Inc.
        (1 for the I_2 Reservoir and
        1 for the Laser Cell)

3) Joulemeters Model PRJ-A, ED-500
    Gentec Inc.

    a) Serial # 18820

    b) Serial # 22890

4) 2 Digital Joulemeters
    Im-2215
    Heathkit

5) Capacitors and Trigger

The remaining 95% of the beam was reflected another 90°. It then passed through a focusing lens and on to a silica wedge.

The silica wedge had a slight angle cut on its front face. The majority of the beam passed through the silica while a small portion was reflected back at an angle off the incident beam. The reflected beam then passed through a pinhole of known size and on to Gentec #3b, a photodiode system. Gentec #3b and the target were one focal length from the focusing lens, and Gentec #3b was used to measure the beam spot size on the target.

Most of the laser beam passed through the silica wedge and on to the target (mirrors). Black paper was placed between the silica wedge and the target to prevent any reflected laser light from striking the mirror. The paper did not interfere with the laser pulse.

The target was mounted in a rigid holder with adjustable "X" (horizontal) and "Y" (vertical) axes. The adjustable axes allowed for controlled separation of each laser shot on a mirror. A Leitz Wetzlar Microscope with a Wild MPS 15 Semiphotomat was used to verify damage both before and after testing with the Iodine laser. Loaded with Polaroid 545 Land film, the Semiphotomat took pictures of several manufactured defects and damage sites on each mirror. The microscope was equipped with a ruler calibrated in microns which was very helpful in measuring the damage spot sizes on the mirrors.

4.2 Calibration of Equipment

Supervised by Major Terry Deaton, Lee Burton calibrated the iodine laser damage equipment in February of 1984.

13

4.2.1. Gentec #3a Calibration

Gentec number 3a, which was used to monitor the energy (J) of the incident iodine laser beam, was calibrated by replacing the target with a Scientech (S-1). The Scientech is a photo diode, the output of which is measured in volts. The output voltage, a measure of the number of photons in the laser pulse, was proportional to the output energy of the laser. Gentec #3a was calibrated using the calculated laser pulse output from the Scientech. For convenience and accuracy a Heathkit digital Joulemeter (IM-2215) was used to convert the analog signal from Gentec #3 to a digital signal.

4.2.2. Gentec #3b Calibration

Gentec #3b was used to measure the beam transmission through a pinhole of known size. This provided the means to calculate laser pulse spot size.

Before the pinhole was present, Gentec #3b was calibrated to correspond with Gentec #3a's laser pulse energy output. This was accomplished by pulsing the iodine laser and then adjusting Gentec #3b to correspond to Gentec #3a. Once the two gentecs were syncronized, a pinhole of known size was placed in the path of the reflected beam between the silica wedge and Gentec #3b.

Gentec #3a measured the laser pulse energy, and Gentec #3b measured the fraction of the laser pulse energy left after passing through a known area. Once the laser beam characteristics are known (Section 4.3), the laser fluence (J/m^2) could be calculated.

14

4.3   Iodine Laser Beam Characteristics

4.3.1   Iodine Laser Beam Profile

The iodine laser beam was assumed to have a Gaussian profile, which has the form

$$I(r) \propto e^{-(r/W)^2} \qquad (1)$$

$I(r)$ is the relative intensity of the laser beam measured at a radius r from the center of the beam. Spot size, W, is the value of r when the beam intensity has dropped to $1/e$ of its value at the center of the beam.[9]

To verify the Gaussian beam profile of the laser beam the target was replaced with a calibrated Gentec monitor and its digital meter. The iodine laser was then shot several times, and the laser energy (J) was recorded after each shot. The laser energy output was then averaged over the number of shots taken. Next, a pinhole of radius 0.99 mm was placed in line with the laser beam. Several shots were made with the pinhole in place. The energy outputs where then averaged. This process was continued with pinholes of 0.75 mm, 0.4955 mm, and 0.254 mm. The above data was then entered into a computer code which fit the data to a Gaussian curve. The Gaussian fit was within acceptable scientific limits.

The shape of the iodine laser beam was confirmed in November of 1984, using a frame grabber and a Vidicon (resembles a television screen). The Vidacon contained 520 picksels × 520 picksels; one Picksel corresponds to a given distance in micrometers. A "picture" was taken of the beam, and the data were computer analyzed. The computer, based

15

on the data from the Vidicon photodiode (T.V.), had many discrete points for the Gaussian fit. The Gaussian beam profile was again verified to be a good approximation for the iodine laser beam.

4.3.2 Iodine Laser Beam Output

There were three ways to control the iodine laser output: varying the voltage the capacitors were charged to, varying the I_6 pressure in the laser cell, and using neutral density filters in the beam path. The capacitors had a maximum capacity of 36 kV, and the I_6 laser cell could be pumped to a maximum of 60 Torr. This produced a maximum laser output fluence of about 1.71 MJ/m^2. This was more than adequate since the 50 percent damage threshold occurred at a fluence of 0.352 MJ/m^2.

The iodine laser output depended on many factors, including 1) how well the laser cell was evacuated, 2) the pressure of the I_6 pumped into the cell, and 3) capacitor voltage. The I_6 cell pressure had to be balanced with the capacitor voltage to obtain the desired fluence. Sometimes increased output was lost due to absorption. As I_6 cell pressure increased so did absorption of the beam in the cell. This was due to the higher molecular density in the cell. The many factors involved in producing a iodine laser shot made it difficult to precisely predict the laser fluence prior to each shot. For each laser pulse, the parameters were adjusted to come as close as possible to the desired fluence.

In order to have an accurate measurement of laser fluence, the laser beam energy and size was measured for each shot, as described earlier. Using the beam energy and size measurements, laser fluence could be accurately calculated after each shot and recorded.

The neutral density filters used to control beam fluence only affected the beam energy. The filters absorbed a fraction of the energy without affecting the beam spot size. Filters were used only when the desired fluence could not be reached by varying previously mentioned parameters.

4.4 Experimental Procedure

Any surface "dirt" was removed by blowing compressed air across the reflective surface of each mirror before it was iodine laser damage tested. The mirror was then placed in the target holder. Each mirror had a "mark" considered the top of the mirror, on its edge. The mark was always at the highest point on the mirror and at a 90° angle to the plane of the table top. The target holder's X and Y coordinates were adjusted so that the first laser shot would impact the center right hand side (as seen when facing the mirrored surface) of the mirror (see Appendix B, Fig. 9).

Any gas that might be present from the previous shot was evacuated from the laser cell: the cell was pumped to a vacuum in the 10 milli Torr range. Next the cell was filled with I_6 gas to 40-60 Torr, depending on the output energy desired. The capacitors were then charged to the desired voltage. The lights were turned off, to prevent background noise on the gentecs. Gentecs were zeroed (with the lights off) in preparation for the next laser shot.

The trigger for the laser was just outside the laser room. With the lights still off, the laser was fired. The door was opened enough to let one person enter the room to read the Gentecs. Once the Gentec

17

readings were recorded, the lights were turned on, and the mirror was examined, by sight, for possible signs of damage. Any sign of damage was noted along with laser pulse number.

The first shot on each mirror was made at an energy level that had a very high probability of damaging the mirror. This produced a large, easily found damage spot which acted as a reference when viewing the mirror under the microscope.

After each laser pulse, sites of possible damage were recorded, along with shot number, X and Y reference coordinates, capacitor voltage, I_6 pressure, the energy output of the laser, and the percent transmission through the pinhole.

The mirror was then moved 0.15 inches (3.81 mm) from the previous shot (to prevent any overlap of damage sites), the laser cell evacuated and filled, the capacitors charged, and the Gentecs reset, as was done for the first shot. This process was used for iodine laser damage testing of mirrors #1, #2, #6, and #7. The rough data is in Appendix B.

5. ANALYSIS OF LASER DAMAGE DATA

5.1 Discussion of Laser Damage Mechanisms

The iodine laser pulses damaged the mirrors because defects in the dielectric coatings absorbed energy from the laser pulses. These defects may have been impurities, dislocations, and/or vacancies in the mirror's SiO_2 and ZrO_2 dielectric coatings. The initial reflectivity measurements give a good indication of the relative number of defects present in each mirror. The fewer defects present, the higher the reflectivity.

Four mirrors were used in the iodine laser damage tests: mirrors #1, #2, #6, and #7 with corresponding reflectivities (as measured by G. Petty at Kirtland Air Force Base) of 0.981, 0.979, 0.825 and 0.969 at 1.315 µm. With a reflectivity of 0.825, mirror #6 has substantially more defects than mirrors #1, #2, and #7; therefore mirror #6 should damage much more easily than the other three mirrors.

Damage to the mirrors could have two causes. At small fluences (when just enough energy is deposited by the beam to cause damage), the area on the mirror hit by the laser pulse would stay in thermal equilibrium over the time of the beam pulse; thus, damage would be due to vaporization removing atoms from the mirror surface.

At very large fluences, too much energy present for the atoms at the target site to reach thermal equilibrium would result in a shock wave over the localized area. The resulting damage would resemble a localized explosion.

19

Examination of the mirrors after the laser damage tests suggests that, at the fluences tested, target site atoms were removed/vaporized while at thermal equilibrium. Pictures of several representative damage sites may be seen in Appendix A. For example, for shot 1 on mirror 1 (Fig. 15), the fluence was 1.709 MJ/m^2, the largest fluence used on any laser shot. The picture taken of the damage shows a very symmetrically circular pattern. There are several alternating SiO_2 and ZrO_2 dielectric coatings visible in the bull's-eye pattern. At this fluence there was enough energy absorbed to displace atoms in all 23 dielectric coatings exposing the Si substrate (the dark circular center).

If the damage had been caused by a "shock wave" the damage site would not have the bull's eye pattern. The damage would propagate in the direction(s) where the lattice is the weakest, the resulting pattern would resemble cracked glass.

The circular bull's-eye pattern could be caused by defect(s) present in the mirror absorbing energy from the front end of the pulse; the absorbed energy would vaporize atoms around the defect, causing the defect to grow. As time elapsed, the rest of the laser pulse would continue the process, propagating the damage down through several dielectric layers and outward. This would lead to the circular damage pattern observed.

Another possibility that would lead to the circular bull's eye pattern is that when the laser pulse first hits the mirror a shock wave is formed. This would cause a propagation of the defect(s) along lines where the lattice is weakest. If the target site recovered thermal

equilibrium, the tail end of the laser pulse would smooth out the rough edges by vaporizing atoms, leaving the circular pattern.

It would be very interesting to correlate damage mechanisms as a function of fluence. However, within the scope of this paper, the important point is whether the mirrors were damaged at the tested fluences.

5.2 DATA ANALYSIS

5.2.1 Organization of Data

Because of the large difference between the reflectivities of mirror #6 (83% at λ = 1.315 μm) and mirrors, #1, #2, and #7 ($\cong$98% at 1.315 μm), mirror #6 was analyzed separately.

There were a total of 109 data points: 81 for mirrors #1, #2, and #7 and 28 data points for mirror #6. The 109 data points had a fluence, range of 0.261 MJ/m^2 to 1.709 MJ/m^2. Each data record represents a discrete fluence and either there was damage or there was not. To figure the probability of damage as a function of fluence, data points were combined into fluence intervals. Average fluence of each interval was calculated, along with the percent damage caused by the laser shots within the interval. An upper fluence level of 0.801 MJ/m^2 was set and all shots at or above this limit were considered to be shot at this fluence. Shots at or above 0.801 MJ/m^2 were sparse and all produced a large damage spot. The remaining 75 shots had a fluence range of 0.261 MJ/m^2 to 0.801 MJ/m^2. Several fluence increment sizes were tried over this range. For each fluence band the weighted average fluence and the percent of damage within the band was calculated. Six different

21

Table 3. Calculated Data Sets for Mirrors #1, #2, and #7

# of Points	Set 1		Set 2		Set 3		Set 4		Set 5		Set 6	
	Ave Fluence (MJ/m²)	% Damage	Ave Fluence (MJ/m²)	% Damage	Ave Fluence (MJ/m²)	% Damage	Ave Fluence (MJ/m²)	% Damage	Ave Fluence (MJ/m²)	% Damage	Ave Fluence (MJ/m²)	% Damage
1	0.316	29.4	0.309	35.7	0.277	00.0	0.277	0.0	0.277	0.0	0.277	0.0
2	0.391	65.4	0.382	57.0	0.353	52.0	0.348	55.0	0.332	42.0	0.327	55.0
3	0.508	80.0	0.492	61.0	0.420	80.0	0.398	60.0	0.371	62.5	0.363	53.8
4	0.604	100.0	0.570	77.8	0.491	85.0	0.480	77.0	0.401	67.0	0.385	60.0
5	0.673*	60.0	0.668*	67.0	0.549	80.0	0.540	73.0	0.438	80.0	0.425	60.0
6	0.801	100.0	0.801	100.0	0.612	100.0	0.601	100.0	0.472	100.0	0.449	67.0
7					0.673*	60.0	0.668*	67.0	0.499	78.0	0.490	80.0
8					0.801	100.0	0.801	100.0	0.539	67.0	0.523	80.0
9									0.572	100.0	0.554	67.0
10									0.613	100.0	0.613	100.0
11									0.668*	50.0	0.658*	50.0
12									0.801	100.0	0.672	100.0
13											0.801	100.0

*Not used in data analysis.

data sets were obtained (see Table 3). Note that there is one data point in each set at about 0.670 MJ/m^2 that deviated drastically. This point was statistically thrown out as an outlier and not used in the function-fitting program.

5.2.2 Fitting the Data

A least squares fit 5/360 Fortran IV program was used to calculate the parameter values for each function fit to the laser damage data. C. Chamot developed the computer program, "ANL E208S-Arbitrary Functional Fit" at Argonne National Laboratory. In addition, the author wrote the subprograms to evaluate the function and to calculate the derivatives of the function that were needed for ANL E208S-Arbitrary Functional Fit.[10]

5.2.2.1 Arctangent Function

After the plotted data points were examined, the following arctangent function was fit to the data:

$$D = C_1 \text{ Arctan } [A(F-K)] + C_2 \tag{2}$$

where D = fractional damage

F = laser pulse fluence

K = 50% damage threshold (to be determined)

A = constant (to be determined)

σ = standard deviation

$C_1 = 1/\pi$, $C_2 = 0.50$

The values for C_1 and C_2 were found by taking the limit of Eq. (2) as F goes to ±∞. This produced two equations with two unknowns. From here it was a simple matter to solve for C_1 and C_2.

Equation (2) was fit to all six data sets in Table 3. An F-test verified that each data set was modeling the same distribution.[11] The best fit came from data set 1, which gave the following equation:

$$D = \frac{1}{\pi} \text{Arctan } [A(F-K)] + 0.50 \pm \sigma \qquad (3)$$

where $A = 16.9 \ \mu m/J$

            $K = 0.361 \ MJ/m^2$

            $\sigma = \pm \ 0.117.$

Based on Eq. (3) the data point at a fluence of 0.673 MJ/m^2 (Data set 1) can be rejected as an "outlier" by forming a confidence interval around expected values at 0.673 MJ/m^2.[12] There is a 99% confidence that 0.60 mirror damage is not a representative data point at the above fluence.

To improve on the results of Eq. (2) a second term was added within the bracket of the arctan term.

$$D = \frac{1}{\pi} \text{Arctan } [A(F-K) + B(F-K)^3] + 0.50 \qquad (4)$$

Equation (4) was then fit to each data set using the least squares fit program. The best fit again came from data set 1, which produced the following equation:

$$D = \frac{1}{\pi} \text{Arctan } [A(F-K) + B(F-K)^3] + 0.50 \pm \sigma \qquad (5)$$

where: $A = 16.9 \ \mu m^2/J$

         $B = 110.0 \ nm^6/J^3$

$$K = 0.361 \ MJ/m^2$$
$$\sigma = 0.109$$

Equation (5) is slightly more accurate (based on standard deviations) than is Eq. (3). To verify that the "B" term was needed in the model, an F-test was performed to test the hypothesis B = 0 vs. B ≠ 0. Using a 99% confidence level the hypothesis could not be rejected, therefore, B ≠ 0. From this result the best arctangent fit to the iodine laser damage data is Eq. (3).

5.2.2.2 Exponential Fit.

After closer examination of the data, an exponential function, of the following form was tried:

$$D = 1 - e^{-A(F-B)} \tag{6}$$

where: A = parameter (to be determined)

F = laser fluence J/m^2

B = cutoff fluence (to be determined) J/m^2

Because of the characteristics of an exponential function "B" represents the minimum damage-causing laser fluence. A cutoff fluence is expected since it seems logical that the mirrors can dissipate a certain amount of absorbed laser energy without sustaining damage.

The parameters of Eq. (6) were found using the least squares fit program. As before the best fit was from data set 1 which gave the results below:

$$D = 1 - e^{-A(F-B)} \pm \sigma \tag{7}$$

25

where $A = 8.60\ \mu m^2/J$

$B = 0.275\ mJ/m^2$

$\sigma = 0.053$

The F-test was performed on the variance of the exponential functions and verified that each data set modeled the same distribution. The exponential model above decreased by over half, the standard deviation of earlier models. The F-test was also used to compare the variance of Eq. (7) to the variance of Eq. (3), and it verified at a 99% confidence level that the variances of Eqs. (7) and (3) are from the same population. Equation (7) has the lower standard deviation, therefore, it is a better model of the laser damage data. Figure 2 shows both models and the data points from data set 1.

5.2.2.3 Mirror 6 Analysis

As stated earlier, mirror #6 damage data was analyzed separately because of its low reflectivity (83%), compared to 98% reflectivity for mirrors #1, #2, and #7. Because of its lower reflectivity, mirror #6 should damage at lower laser fluences than the other mirrors: the lower reflectivity indicates the presence of excessive (relatively speaking) defects in the SiO_2 and ZrO_2 dielectric coating. With more defects present, the mirror will absorb a larger portion of the laser beam energy, as a consequence, the mirror will damage at lower fluences.

The data, which consisted of 28 points, was grouped into fluence intervals as before. The best fit for both the Arctan and exponential functions came from the following data set.

Figure 2. Models of Iodine Laser Damage Data for Mirrors #1, #2, and #7.

$D = 1 - e^{-8.60(F-0.275)} \pm 0.053$

$D = 1/\pi \; \text{Tan}^{-1}[16.90(F-0.361] + 1/2 \pm 0.117$

△ Data points

Shaded area is region of significant fit

Iodine Laser Fluence (MJ/m^2)

Fractional Damage

27
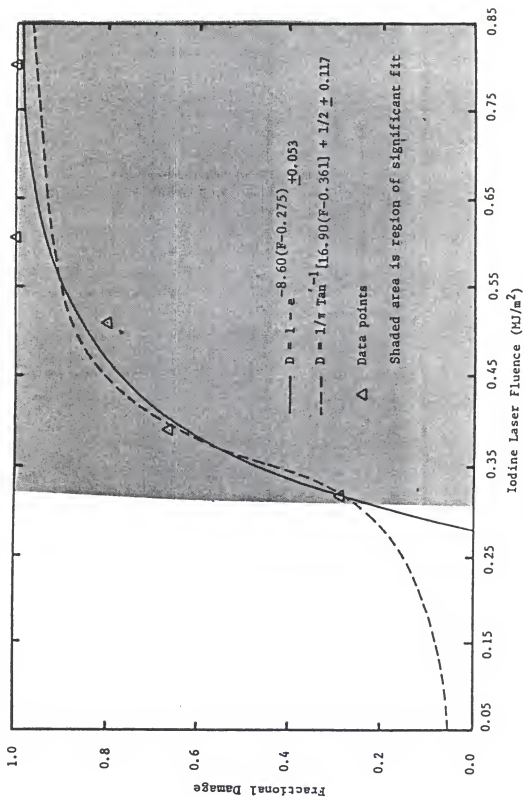
Table 4. Data From Mirror #6.

Fluence (MJ/m^2)	Fractional Damage
0.285	0.54
0.322	0.73
0.389	1.00

From the above data the Arctan function became:

$$D = \frac{1}{\pi} \text{Arctan } [A(F-K)] + 0.50 \pm \sigma \qquad (8)$$

$$A = 27.60 \ \mu m^2/J$$

$$K = 0.278 \ MJ/cm^2$$

$$\sigma = 0.115$$

Equation (8) was expanded to the form of Eq. (4), but as before the hypothesis that B = 0 was accepted.

The exponential model to mirror #6 data follows:

$$D = 1 - e^{-A(F-B)} \qquad (9)$$

$$\text{where: } A = 19.8 \ \mu m^2/J$$

$$B = 0.247 \ MJ/m^2$$

$$\sigma = 0.077$$

Based on an F-test, Eqs. (8) and (9) were found to model the same distribution. Each model can be seen in Fig. 3.

5.3 DATA RESULTS ANALYSIS

5.3.1 Mirrors #1, #2, and #7 Results

Based on Fig. 2 the exponential model (Eq. 7) and the arctangent model (Eq. 3) are very similar at fluences above 0.310 MJ/m^2. This is

28

Figure 3. Models of Iodine Laser Damage Data for Mirror #6.

$D = 1 - e^{-19.8(F-0.247)} \pm 0.077$

$D = 1/\pi \, Tan^{-1}[27.60(F-0.27)] + 1/2 \pm 0.115$

△ Data points

Shaded area is region of significant fit

Iodine Laser Fluence (MJ/m²)

Fractional Damage

29
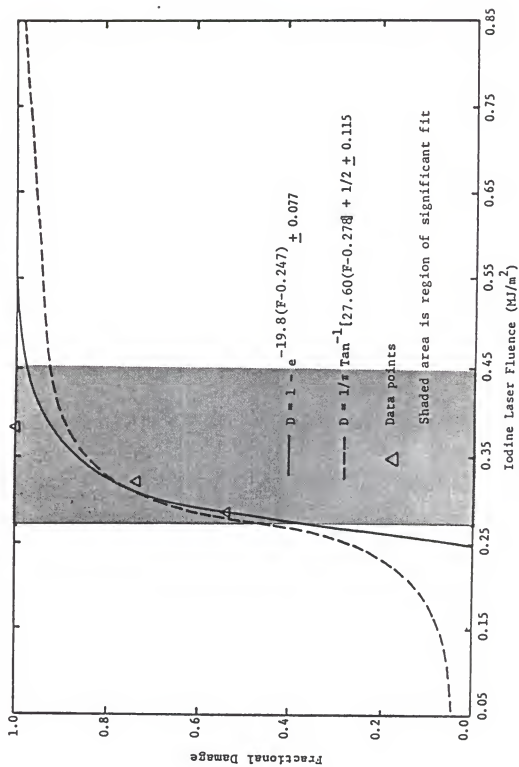
emphasized by the 50 percent damage threshold value calculated from each function. Equation (7) predicts a 50% damage threshold of $(0.355 \pm .015)$ MJ/m^2 and Eq. (3) predicts a threshold of $(0.361 \pm .014)$ MJ/m^2. This is only a 1.7% difference.

With no data points below 0.300 MJ/m^2, where the arctangent and exponential functions differ the most, it is hard to judge which model is more representative of the data. Both models have been verified to model the same distribution.

The exponential model predicts a minimum damage threshold of $(0.275 \pm .015)$ MJ/m^2, which physically makes sense. It also has the lower standard deviation.

In contrast, the arctangent model predicts that 19.11% of the time a fluence of 0.275 MJ/m^2 will damage the mirror. Even at a fluence of 0.050 MJ/m^2 the arctangent model predicts damage 6% of the time. Though 6% is small, it is significant when compared to zero damage predicted by the exponential model.

5.3.2 Mirror 6 Results

Based on Fig. 3 both models fit the data at laser fluences above $(0.270 \pm .011)$ MJ/m^2. The arctangent (Eq. 8) predicted a 50% damage threshold of (0.278 ± 0.008) MJ/m^2 whereas the exponential function (Eq. 9) predicted a value of 0.282 MJ/m^2, a difference of 1.42%. Equation (9) also predicted a minimum damage threshold of $(0.247 \pm .007)$ MJ/m^2.

5.3.3 Effects of Reflectivity on Damage Threshold

As stated earlier, mirrors with low reflectivities, that is, with more defects (dislocations and impurities) are expected to damage easier: not only is less light reflected but there are more sites for the energy to be absorbed.

Compared, Figs. 2 and 3 show that lower reflectivity resulted in greater laser damage, as was predicted. As reflectivity went from 98% to 83% the 50% laser damage threshold went from $(0.355 \pm .015)$ MJ/m^2 to $(0.282 \pm .008)$ MJ/m^2 a change of 20.56%.[a] The minimum laser damage threshold also changed from $(0.275 \pm .015)$ MJ/m^2 to $(0.247 \pm .007)$ MJ/m^2, a change of 10.18%. These changes lead to the following conclusions.

Because the 50% damage threshold decreased almost twice as much as the minimum damage threshold, the initial slope of the exponential increased dramatically (see Fig. 3). Consequently, at lower reflectivity, the mirror damages very easily. As an example, a mirror with 98% reflectivity will damage approximately 48% of the time at a fluence of 0.350 MJ/m^2. A mirror with 83% reflectivity would damage 87.0% of the time. A difference of 44.8%.

The results also strengthen the theory that a minimum fluence (the minimum amount of absorbable energy) is needed to induce damage to the SiO$_2$ and ZrO$_2$ mirror coating.

---

[a]The exponential function will be the basis for calculations in the discussion of reflectivity effects on laser damage.

If mirrors with reflectivity less then 83% were tested, the exponential curve would probably approach a vertical asymtope very quickly. The lower reflectivity would also cause the damage curve to shift to the left. This shift would be the result of a decrease of the minimum damage threshold. As the exponential curve approached a vertical asymtope, the minimum damage threshold should approach its lower limit.

6. NEUTRON DAMAGE TEST

6.1 Introduction

Iodine mirrors must resist neutron-induced damage; during Strategic Defense Initiative use these mirrors may be exposed to the detonation of nuclear weapons. Neutrons, because of their potential to cause permanent damage, would certainly represent a significant portion of the radiation the system would have to withstand.

If the mirrors are used in an inertial confinement fusion system, they would have the potential to be exposed to a neutron flux. In both applications the neutrons could have several MeV of energy when they reach the mirror. If even a fraction of this energy is imparted to a primary knock-on atom, the mirror would be greatly damaged.

Though neutrons are not the only type of radiation present in the environment of a SDI or a ICF system, it will be the only radiation source present in this experiment. It will be much easier to model more complicated radiation environments if the damage from each specific type of radiation present is understood.

6.1.1 Neutron Damage Mechanisms

Iodine mirrors can be damaged from exposure to a neutron flux depending upon several parameters, including the energy of the neutrons, the density of the flux, and exposure time. Neutrons can cause four types of damage. First, a neutron flux can create Frenkel and Schotty defects, which would increase the number of color-center sites. Second, it can create secondary ionization, which would also lead to color-center activation. Third, at high neutron fluences, lattice-

33

vacancy clustering is possible; this would cause flaking of the thin SiO_2 and ZrO_2 dielectric coatings. Fourth, primary knock-on atoms could cause massive displacement of lattice atoms in the dielectric coatings or the mirror substrate; massive displacement of lattice atoms in the SiO_2 and ZrO_2 dielectric coatings might cause a phase shift in the reflectivity curve of the mirror.

6.2 Methodology

Iodine laser mirrors #11 and #12 were selected to be irradiated with neutrons. They had a maximum reflectivity at $\lambda = 1.315$ μm of 0.987 and .981 respectively.

The two mirrors were transported to the Clinton P. Anderson Meson Physics Facility at Los Alamos, New Mexico for irradiation in the LAMPF Beam Stop. Each mirror was placed in a prefabricated aluminum case to protect the mirror surfaces. The aluminum case is shown in Appendix C, Fig. 10.

The mirrors, each enclosed in an aluminum case, were placed in the #12 box in the neutron irradiation target area. See Figures in Appendix C. The two mirrors were then exposed to a spallation neutron fluence of 1.5×10^{22} neutrons/m^2. Figure 14 shows the energy distribution for the neutrons that irradiated the A-6 target station, which includes neutron irradiation box 12.

The two aluminum cases were removed from the beam stop after irradiation and the mirrors were removed from the cases.

The reflectivity curve of each mirror was then remeasured using the procedure described in section 3.2. Because of the extensive damage

that was visible to each mirror surface, the reflectivity was measured at six different orientations: at 0°, 60°, 120°, 180°, 240° and 300° with respect to the "top of the mirror" (described earlier). The six reflectivity measurements were then averaged. The result was a reflectivity of .647 for mirror #11 and .783 for mirror #12 (measured at $\lambda = 1.315$ μm).

6.3 Discussion of Results

Extensive damage was visible on both mirrors. The dielectric coatings had begun flaking away. The large amount of flaking on both mirrors suggests that, over the neutron fluence and energy range tested, there were massive displacements and/or lattice vacancy clustering.

Mirror #11's reflectivity decreased by 34.5% and mirror #12's reflectivity decreased by 20.2% (see Fig. 4). These are significant drops in reflectivity, considering that these mirrors would have to function in high-power and high-energy-density laser systems, where a small reflectivity reduction would lead to catastrophic system failure.

Though it was not possible to iodine laser damage test mirrors #11 and #12 after neutron irradiation, they would probably have an even lower 50% damage threshold than did mirror #6 based on the final reflectivity measurements.

From the above results it appears that, in either an SDI or an ICF system, the iodine mirrors, as presently manufactured, could not remain functional after exposure to a neutron environment similar to the one created during the test.

Figure 4. Post Neutron Irradiation Reflectivity of Mirrors #11 and 12.

Fractional Reflectivity

Wavelength (nm)

—— Typical Preirradiation Reflectivity

– – – Post Neutron Reflectivity of Mirror #12

–·–·– Post Neutron Reflectivity of Mirror #11
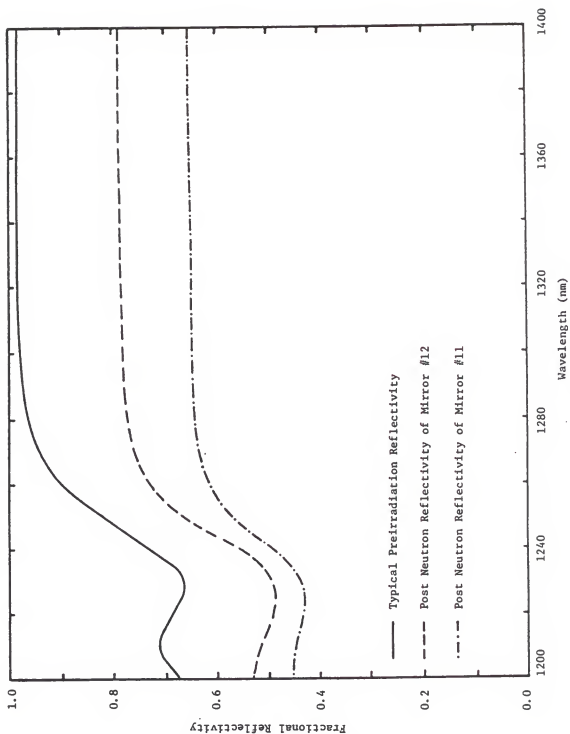
The results of the neutron damage experiment were instrumental in explaining optical damage to mirrors used in the 20 MeV free electron laser at Los Alamos National Laboratory.[13] Neutrons, created by photonuclear reactions, were continuously damaging the optical coated mirrors, reducing their optical properties. As a result of the neutron damage, mirrors in the free electron laser had to be replaced regularly. The working lifetime of the mirrors in the free electron laser have been substantially increased by replacing the optical coated mirrors with metal coated mirrors.

7. GAMMA-RAY DAMAGE TEST

7.1 Introduction

The nature of the systems for which the iodine laser mirrors were designed require the mirrors to stand up in a radiation environment. Either the SDI or the ICF system could be exposed to a substantial dose of gamma-ray irradiation. Gamma irradiation presents a much larger problem to the components of the SDI system due to the nature of atomic explosions.

Without careful planning, the mirrors in an ICF system could also become gamma irradiated, the result of a neutron interacting with matter via a (n,γ) reaction. Assuming deuterium and tritium are used as the fusion material, the product of the fusion reaction is a helium atom leaving a 14 MeV neutron.[9] As the neutron thermalizes, it is likely to interact with matter.

7.2 Methodology

To correlate gamma-ray dose to iodine-laser mirror damage, four mirrors were exposed to a range of gamma doses.

A Gammacell-220 manufactured by Atomic Energy of Canada Ltd. was used to irradiate the four mirrors. The Gammacell contained 3.963 kCi (146.63TBq) of ^{60}Co on March 15, 1965. The irradiation chamber was 6 inches in diameter and 8 inches high. A Plunger moved the irradiation chamber into the middle of the source upon command. An electronic timer with hours, minutes, and seconds settings automatically removed the chamber from the source when time expired.

Mirrors #3, #4, #5, and #8 were chosen to receive gamma-ray doses of 0.5 Mrad (5.0 kGy), 1.0 Mrad (10.0 kGy), 2.0 Mrad (20.0 kGy), and 5.0 Mrad (50.0 kGy) respectively. The dose rate was approximately 21.76 krad/h (217.6 Gy/h).

To place the four mirrors in the center of the gamma irradiation a $3\frac{1}{2}$ inch tall wooden block was made to fit into the center of the irradiation chamber. The mirrors were then stacked on the wooden block. Mirror #8 was on the bottom, followed by #5, #4, with #3 on the top. The stack was directly in the center of the chamber. Since the chamber was placed in the source's center (with no irradiation from top or bottom), the mirrors were evenly exposed. The exposure times and doses are shown in Table 5.

TABLE 5. SiO_2 + ZrO_2 on Si Substrate Mirrors
Gamma-Ray Doses

Mirror	Exposure Time (hr)	Dose*	
		(Mrad)	(kGy)
3	23.0	0.501	5.01
4	46.0	1.001	10.01
5	92.0	2.002	20.02
8	230.0	5.005	50.05

*Dose calculated based on ^{60}Co
activity as of 10/26/85

Once all four mirrors had been irradiated for the designated time, they were taken to the Air Force Weapons Laboratory. Non-irradiated mirrors #9 and #10 were taken for comparison. (Note that the iodine laser mirrors had been manufactured approximately 1.3 years prior to this

test. In addition, mirrors #9 and #10 have never been exposed to any type of radiation other than ever-present background radiation).

After irradiation, reflectivity curves for these six mirrors were measured at angles of 0°, 120°, and 240° (as described earlier) from 900 nm to 1500 nm. These reflectivity curves were averaged and then compared to the reflectivity curves made shortly after the mirrors were produced.

7.3 Discussion of Results

There was one unexpected test result. For 1.3 years, mirrors #9 and #10 were stored in the protective plastic cases they were shipped in. They were never involved in any type of radiation test, yet, in those 1.3 years, the reflectivity of the two unirradiated mirrors, #9 and #10, dropped by over 11% (λ = 1.315 μm). The reflectivity curves of mirrors #9 and #10 can be seen in Appendix D.

With 20/20 hindsight, one of the objectives of the research should have included determining aging effects.

Figures 15-18 compare the reflectivity curves of mirrors #3, #4, #5 and #8 before and after gamma irradiation. In each case the reflectivity at 1.315 μm decreased by an average of 15.02%. Also, in each case, at the lower wavelengths the reflectivity curves shifted toward the ultraviolet.

An interesting result is that figures 15-18 are very similar. Though the gamma doses varied from 0.5 Mrad (5.0 KGy) to 5.0 Mrad (50.0 kGy), the drop in reflectivity at 1.315 μm was between 13.38% (for mirror 4) to 16.94% (for mirror 8). A larger difference might have been expected considering the range of doses.

40

From the above data, it appears that aging alone will significantly effect the efficiency of the mirrors. The unirradiated mirrors exhibited the same ultraviolet phase shift as the gamma irradiated mirrors. The unirradiated mirrors reflectivity also decreased at 1.315 μm. Decreases in reflectivity of 11.94% and 11.73% were found for mirrors #9 and #10, respectively (shown in Figures 19 and 20).

The initial reflectivity curves were measured in July, 1984, and the second reflectivity curves were measured in October 1985. Of the six mirrors, mirrors #3, #4, #5, and #8 were exposed to gamma irradiation just prior to the second measurement; mirrors #9 and #10 were not irradiated. The test data leads to two conclusions.

One, as the mirrors age their reflectivity deteriorates. The mirrors lose their high efficiency at the designed, 1.315 μm wavelength. This reflectivity loss is accompanied by a shift in the reflectivity spectrum of each mirror toward the U.V. and can be detected at about 1230 nm.

One hypothesis about the cause of the aging-related phase shift is that the SiO_2 and/or ZrO_2 dielectric coatings are either giving up or absorbing oxygen.

Two, gamma ray doses to 5 Mrad (50 kGy) appear to have very little permanent effect on the optical characteristics of the mirrors compared to aging. When the percent of reflectivity change is averaged and a 95% confidence interval is formed around the average change of 13.96% for all six mirrors, upper and lower limits of 19.50% and 8.41% are found. So, though all the gamma irradiated mirrors showed a slightly larger decrease in reflectivity, the larger decrease can not be

41

distinguished statistically. This may be due to the small population size. It may also be influenced by the fact that the mirrors were not gamma irradiated right after their production; time-lapse (over a year) may alter the effects gamma radiation has on the mirrors.

TABLE 6. Results of Gamma-Ray Experiment

| Mirror | Dose | | Reflectivity[*] | | Percent |
	(Mrad)	(kGy)	(July 1984)	(Oct 1985)	Decrease
3	0.50	5.00	0.958	0.815	14.93
4	1.001	10.01	0.942	0.816	13.38
5	2.002	20.02	0.959	0.817	14.81
8	5.005	50.05	0.986	0.819	16.94
9	--	--	0.930	0.819	11.94
10	--	--	0.946	0.835	11.73

[*]Measured at a wavelength of 1.315 μm.

8. SUMMARY OF RESULTS

8.1 Iodine Laser Damage Test Results

An exponential function predicted the probability of damage best for the (SiO_2 + ZrO_2 on Si substrate) mirrors when shot with an iodine laser (= 1.315 m) up to fluences of 1.70 MJ/m^2. Iodine laser damage data obtained from mirrors that were approximately 98% reflective at a wavelength of 1.315 m were best modeled by the equation:

$$D = 1 - e^{-A(F-B)} \pm \qquad (10)$$

where D = predicted fractional damage

F = the laser fluence (J/m^2)

A = 0.60 m^2/J

B = 0.275 MJ/m^2

 = 0.053

Equation (10) predicts a 50% damage threshold at (0.355 ± .015) MJ/m^2 and a minimum damage threshold of (0.275 ± .015) MJ/m^2.

For the iodine laser mirror tested with a reflectivity of 83% at a wavelength of 1.315 m, the following exponential function best predicted the damage data:

$$D = 1 - e^{-A(F-B)} \pm \qquad (11)$$

F = the laser fluence (J/m^2)

A = 19.8 m^2/J

B = 0.247 MJ/m^2

 = 0.077

For mirrors with an 83% reflectivity, Eq. (11) predicted a 50% damage threshold of $(0.282 \pm .008)$ MJ/m^2 and a minimum damage threshold of $(0.247 \pm .007)$ MJ/m^2.

8.2 Neutron Irradiation Results

Mirrors #11 and #12, which were exposed to a spallation neutron fluence of 1.5×10^{22} neutrons/m^2 were extensively damaged. The SiO$_2$ and ZrO$_2$ dielectric coatings flaked, and there was a measured decrease in reflectivity. At the 1.315 m design wavelength, the reflectivity dropped to 0.647 (34.5% decrease) for mirror #11 and to 0.783 (20.2% decrease) for mirror #12.

8.3 Gamma-Ray Irradiation Results

Mirrors #3, #4, #5 and #8 were irradiated with gamma-rays using a ^{60}Co source to doses of 0.5 Mrad (5.0 kGy), 1.0 Mrad (10.0 kGy), 2.0 Mrad (20.0 kGy), 5.0 Mrad (50.0 kGy), respectively. When the irradiated mirrors' reflectivity spectra were measured the spectra for control mirrors #9 and #10 were remeasured. The irradiated mirrors phase-shifted toward the U.V., with an average drop in reflectivity of 15.02% ($= 1.315$ m). The two unirradiated mirrors had identical phase shifts toward the U.V. and an average drop in reflectivity of 11.84% ($= 1.315$ m). Aging appears to have caused the phase shifts of all six mirrors. Though the irradiated mirrors had a slightly larger decrease in reflectivity, this decrease could not be statistically distinguished from the population mean. This is probably due to the small sample size.

9. CONCLUSIONS

Based on the results of the gamma irradiation, these particular mirrors should not be used for long term applications. The "aging" problem limits long term application possibilities, although they may be resolved with examination of the manufacturing techniques. The SiO_2 and ZrO_2 dielectric coatings procedure should also be scrutinized: atoms could be diffusing to and from each dielectric coatings and to and from the air.

For some short term applications the mirror may work fine. At laser fluences less than or equal to $(0.275 \pm .015)$ MJ/m^2, mirrors with 98% reflectivity at $\lambda = 1.315$ μm) are not damaged. Even with a gamma environment, the mirrors may remain functional after doses of 5 Mrad (50 kGy). Of course, mirror functional lifetime will depend on the system environment and the requirements that the system puts on the mirror.

According to the neutron test, the mirrors cannot function efficiently in an environment with a neutron fluence of 1.5×10^{22} neutrons/m^2.

These mirrors are very impractical for the ICF and SDI systems they are being considered for. Both systems need to maximize output energy to accomplish their goals. A minimum damage threshold of $(0.275 \pm .015)$ MJ/m^2 would severely limit either system. Furthermore, this minimum damage threshold will be decreasing with time, further limiting the system efficiency. The minimum damage threshold will decrease even faster in a radiation environment putting further strain on the system.

46

It might be possible to use the mirrors in an ICF system and replacing them when their efficiency dropped below the required specifications. This would require periodic downtime which is generally undesirable. This is also true for earth based SDI systems which are easily accessible (compared to space based SDI systems).

The (SiO_2 + ZrO_2 on Si substrate) mirrors main contribution to ICF and SDI systems will be from the results of tests performed on them. The results will lead to better manufacturing materials and techniques. The (SiO_2 + ZrO_2 on Si substrate) iodine laser mirrors provide a starting point from which improvements can be made. The significance of a starting point should not be overlooked, for the journey of a thousand miles starts with the first step.

10. RECOMMENDED SCOPE FOR FUTURE WORK

As with many research projects, more questions were raised here than were answered. Several follow-ups using the iodine laser that would be very interesting. As a logical follow-up, the mirrors should be exposed to neutrons and gamma-rays to determine the mirrors' 50% and minimum damage thresholds. These results could be compared to the iodine laser damage results for mirrors #1, #2, #6, and #7. More testing will require the production of new mirrors.

Another interesting experiment would be to regularly and systematically monitor the aging effects on the reflectivity spectra: it would seem that the mirrors' reflectivity spectra would eventually stabilize. Such monitoring could determine how long it takes, how much drop in the reflectivity there is, and how much shift the initial reflectivity spectrum shifts.

Possible experiments with neutrons and gamma-rays are endless. Pertinent questions about this set of mirrors could be answered by testing several mirrors at neutron fluences above and below 1.5×10^{22} neutrons/m^2. Tests with a wide range of fluences could give a function that could be fit to the data as was done with the laser damage data.

The same could be done for gamma ray doses above 5 Mrad (50 kGy). Studying the transient gamma ray on the mirrors could provide valuable information. Such an experiment requires sychronizing the reflectivity measurements within the time period the dose is received. This is the

topic of Kevin Stroh's and Gary Scronce's research paper at Kansas State University, Transient Gamma Ray Effects. With the above information a more complete analysis of the mirrors could be accomplished. This would make it much easier to compare changes in the manufacturing process or materials used to produce the mirrors.

Once data and results are available for wide ranges of doses and fluences, the more interesting and more typical radiation environments can be tested. This would be an important milestone, especially for SDI systems. To produce a reliable SDI system, the complicated radiation environments that they may be encountered need to be understood.

11. ACKNOWLEDGEMENTS

12. LITERATURE CITED

1. P.J. Brannon and R.W. Morris, "Radiation Inducted Absorption in Optical Materials," Sandia National Laboratories, Jan. 85, prepared for U.S.D.O.E.

2. Donald F. Heath and Paul A. Sacher, "Effects of a Simulated High-Energy Space Environment on the Ultraviolet Transmittance of Optical Materials Between 1500A and 3000A", Applied Optics, Vol. 5, No. 6, June 1966.

3. Dr. H. Donnert, FJSRL and KSU, Private Communication.

4. Gary Scronce, FJSRL and KSU Graduate Student, Private Communication.

5. Kevin Stroh, FJSRL and KSU Graduate Student, Private Communication.

6. P.J. Braunon and R.A. Hamil, Sandia National Laboratories, Private Communication.

7. D. Boucher, Ed., "Optical Fibers in Adverse Environments", SPIE Report, Vol. 404, 1983.

8. J.O. Porteus, "Determination of the Onset of Defect-Drive Pulsed Laser Damage in 2.7 μm Optical Coatings (U)", Michelson Laboratory, Naval Weapons Center, China Lake, California.

9. Donald C. O'Shea, W. Russell Callen, and William T. Rhodes, Introduction to Lasers and Their Applications, Addison-Wesley Publishing Co. (1977).

10. K. Szabo, "ANL E208S-Arbitrary Functional Fit," System/360 Library Routine, Argonne National Laboratory, Argonne, Illinois.

11. Christopher Chatfield, Statistics for Technology, Great Britain, J.W. Arrowsmith, Ltd. (1978).

12. John Boyer, Regression and Correlation, KSU class notes for Statistics 705.

13. Brian Newnam, Private Communication, 1985.

13. APPENDICES

Photographs of Iodine Laser Damage to

(SiO_2 + ZrO_2 on Si Substrate) Mirrors

Figure 5.   Iodine Laser Damage to SiO_2 + SrO_2 on Si Substrate Mirrors
            Caused by Iodine Laser λ = 1.315 μm.   Magnification 400×.
            Mirror #1, Shot 1 fluence 1.709 mJ/m^2.
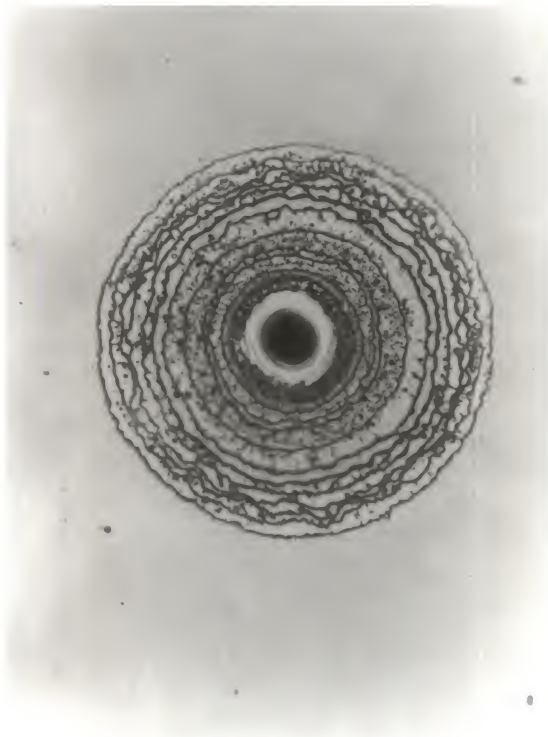
Figure 6. Damage to SiO_2 + SrO_2 on Si Substrate Mirror Caused by Iodine Laser λ = 1.315 μm. Magnification 400×. Mirror #2 Top: Shot 14, fluence 0.489 mJ/m^2. Bottom: Shot 25, fluence 0.395 mJ/m^2.
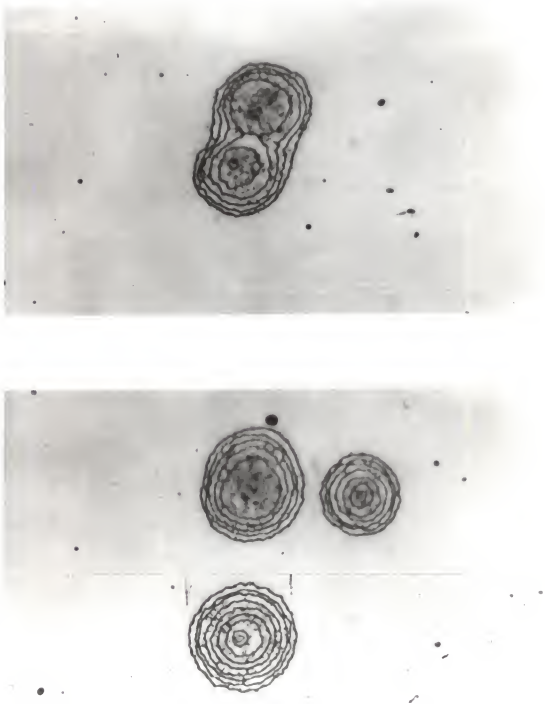
Figure 7. Damage to SiO_2 + SrO_2 on Si Substrate Mirror Caused by Iodine Laser λ = 1.315 µm. Magnification 400×. Mirror #7. Top: Shot #19, fluence 0.328 mJ/m^2. Bottom: Shot #9, fluence 375 mJ/m^2.

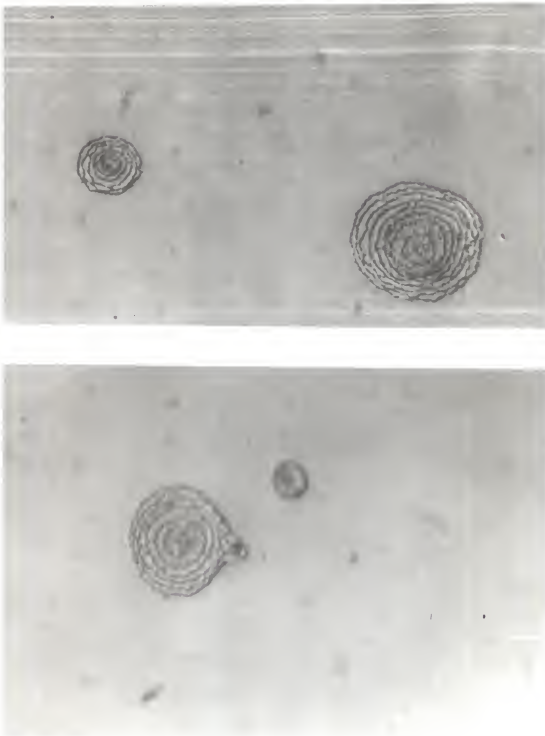Figure 8. Manufactured Defects to SiO_2 + SrO_2 on Si Substrate Mirrors, Magnification 400×. Top: Mirror #1 located by shot #4. Bottom: Mirror #7 located by shot #29.
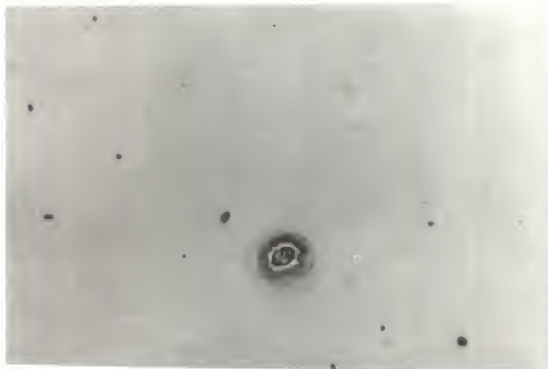
13.2 APPENDIX B

IODINE LASER DAMAGE TESTS

ROUGH DATA

Table 7. Rough Data for Iodine Laser Damage Tests on Mirror #1.

SHOT	POSITION		$(kV)^a$	$LASER_b$ (Torr)	MJ/m^{2c}	$TRANS^d$ %	$Damage^e$
	X	Y					
1	.9	.20	36	60	1.709	20.98	yes
2	1.05	.20	32	55	1.206	21.58	yes
3	1.20	.20	28	40	0.911	23.88	yes
4	1.35	.20	28	40	0.278	19.12	no
5	1.50	.20	28	40	0.543	20.60	no
6	1.65	.20	28	40	0.549	20.75	yes
7	1.6	.35	28	40	0.543	20.06	no
8	1.45	.35	28	40	0.549	19.69	yes
9	1.30	.35	28	40	0.529	21.12	yes
10	1.15	.35	34	60	0.509	20.92	yes
11	1.00	.35	32	55	0.436	19.48	yes
12	1.00	.50	32	55	0.409	18.89	no
13	1.15	.50	32	55	0.429	19.95	yes
14	1.30	.50	32	55	0.442	20.17	no
15	1.45	.50	32	55	0.409	19.48	yes
16	1.60	.05	34	60	0.476	19.20	yes
17	1.45	.05	34	60	0.503	19.50	no
18	1.30	.05	34	60	0.496	19.67	yes
19	1.15	.05	34	60	0.482	19.47	yes
20	1.00	.05	30	45	0.348	18.97	no
21	1.05	-.10	30	45	0.348	19.27	no
22	1.20	-.10	30	45	0.670	20.64	no
23	1.35	-.10	30	45	0.663	20.17	no
24	1.50	-.10	30	45	0.683	23.65	yes

a. Voltage the capicators were charged to.

b. I_6 pressure in the laser cell.

c. Measured output energy and beam size to calculate fluence.

d. Measured transmission through pinhole.

e. Damage verified under microscope.

Table 8. Rough Data for Iodine Laser Damage Tests on Mirror #2.

SHOT	POSITION X	Y	$(kV)^a$	LASER (Torr)^b	MJ/m^2 ^{c}	TRANS^d %	Damage^e
1	.9	.9	34	60	0.797	18.6	yes
2	1.05	.9	34	60	0.771	19.4	yes
3	1.20	.9	32	55	0.690	19.3	yes
4	1.35	.9	32	55	0.616	18.6	yes
5	1.50	.9	32	55	0.657	19.2	yes
6	1.65	.9	32	55	0.610	18.2	yes
7	1.75	.9	32	55	0.643	19.5	yes
8	1.70	1.05	30	45	0.570	16.0	yes
9	1.55	1.05	30	45	0.576	19.5	yes
10	1.40	1.05	30	45	0.570	19.7	yes
11	1.25	1.05	28	45	0.489	19.0	no
12	1.10	1.05	28	45	0.503	23.7	yes
13	.95	1.05	28	45	0.516	19.7	yes
14	1.00	.75	28	45	0.489	19.9	yes
15	1.15	.75	28	45	0.476	20.4	yes
16	1.30	.75	36	65	0.456	19.7	yes
17	1.45	.75	35	63	0.449	19.9	yes
18	1.60	.75	34	60	0.375	20.2	yes
19	1.75	.75	34	60	0.369	20.1	yes
20	1.60	.60	34	60	0.382	18.6	yes
21	1.45	.60	32	55	0.389	18.3	yes
22	1.30	.60	32	55	0.395	18.9	yes
23	1.15	.60	32	55	0.382	19.2	no
24	1.15	1.20	32	55	0.369	19.3	yes
25	1.30	1.20	32	55	0.395	20.0	yes
26	1.45	1.20	32	55	0.382	19.7	no
27	1.60	1.20	32	55	0.369	17.3	no
28	1.30	1.35	32	55	0.375	19.4	no

a. Voltage the capicators were charged to.

b. I_6 pressure in the laser cell.

c. Measured output energy and beam size to calculate fluence.

d. Measured transmission through pinhole.

e. Damage verified under microscope.

Table 9. Rough Data for Iodine Laser Damage Test on Mirror #6.

SHOT	POSITION X	POSITION Y	(kV)[a]	LASER (Torr)[b]	MJ/m^2[c]	TRANS % [d]	Damage[e]
1	.4	.50	32	55	1.092	21.2	yes
2	.55	.50	32	55	0.362	19.8	yes
3	.70	.50	32	55	0.342	19.1	yes
4	.85	.50	32	55	0.348	19.0	yes
5	1.00	.50	32	55	0.355	22.8	no
6	1.15	.50	32	55	0.355	18.5	yes
7	1.10	.65	30	45	0.308	19.8	no
8	.95	.65	30	45	0.302	20.0	no
9	.80	.65	30	45	0.295	19.8	no
10	.65	.65	30	45	0.295	23.8	yes
11	.50	.65	34	60	0.362	20.7	yes
12	.35	.65	34	60	0.369	18.0	yes
13	.45	.80	34	60	0.389	18.9	yes
14	.60	.80	34	60	0.369	17.7	yes
15	.75	.80	34	60	0.382	18.0	yes
16	.90	.80	34	60	0.395	18.8	yes
17	1.05	.80	33	40	0.369	20.0	no
18	.80	.95	28	40	0.268	19.2	yes
19	.65	.95	28	40	0.261	19.6	no
20	.35	.40	28	40	0.248	22.3	no
21	.50	.40	28	40	0.248	21.6	no
22	.65	.40	31	50	0.302	19.6	yes
23	.80	.40	32	55	0.315	20.8	yes
24	.95	.40	32	55	0.288	17.1	no
25	1.00	.20	32	55	0.295	17.6	yes
26	.85	.20	32	55	0.295	17.4	yes
27	.70	.20	32	55	0.295	17.2	yes
28	.55	.20	32	55	0.302	17.2	yes

a. Voltage the capicators were charged to.

b. I_6 pressure in the laser cell.

c. Measured output energy and beam size to calculate fluence.

d. Measured transmission through pinhole.

e. Damage verified under microscope.

Table 10. Rough Data for Iodine Laser Damage Test on Mirror #7.

SHOT	POSITION		$(kV)^a$	LASER $(Torr)^b$	MJ/m^{2c}	TRANS^d %	Damage^e
	X	Y					
1	.60	.50	28	40	0.838	22.42	yes
2	.75	.50	28	40	0.536	21.42	yes
3	.90	.50	34	60	0.402	18.12	yes
4	1.05	.50	34	60	0.375	17.19	yes
5	1.20	.50	34	60	0.369	16.79	no
6	1.35	.50	34	60	0.375	17.19	yes
7	1.35	.65	34	60	0.369	17.08	no
8	1.20	.65	34	60	0.415	19.48	yes
9	1.05	.65	34	60	0.375	17.58	yes
10	.90	.65	32	55	0.362	18.93	yes
11	.75	.65	32	55	0.348	18.97	no
12	.60	.65	32	55	0.369	19.80	yes
13	.70	.80	32	55	0.355	19.33	yes
14	.85	.80	32	55	0.369	20.06	yes
15	1.00	.80	32	55	0.395	21.10	no
16	1.15	.80	32	55	0.369	20.06	yes
17	1.30	.80	30	45	0.395	20.60	yes
18	1.10	.95	30	45	0.369	20.07	yes
19	.95	.95	30	45	0.328	20.54	yes
20	.80	.95	30	45	0.322	20.48	no
21	.65	.35	30	45	0.322	20.38	yes
22	.80	.35	30	45	0.328	20.17	no
23	.95	.35	28	40	0.275	19.55	no
24	1.10	.35	28	40	0.281	23.06	no
25	1.25	.35	28	40	0.281	23.52	no
26	1.20	.20	29	43	0.268	20.32	no
27	1.05	.20	30	45	0.328	22.57	no
28	.90	.20	30	45	0.328	20.02	yes
29	.75	.20	30	45	0.335	20.43	no

a. Voltage the capicators were charged to.

b. I_6 pressure in the laser cell.

c. Measured output energy and beam size to calculate fluence.

d. Measured transmission through pinhole.

e. Damage verified under microscope.

Figure 9. Shot Placement for Iodine Laser Damage Tests.

Mirror #1

```
       15   14   13   12

    7   8    9   10   11

  6   5    4   3   2    1

16   17   18   19   20

    24   23   22   21
```

Mirror #2.

```
                28

         27   26   25   24

   8   9   10   11   12   13

   7   6    5    4    3    2    1

19   18   17   16   15   14

         20   21   22   23
```

Mirror #6

```
          18   19

17   16   15   14   13

7   8    9   10   11   12

  6   5    4   3   2    1

24   23   22   21   20

     25   26   27   28
```

Mirror #7

```
          18   19   20

17   16   15   14   13

7   8    9   10   11   12

  6   5    4   3   2    1

25   24   23   22   21

     26   27   28   29
```

13.3 APPENDIX C

A-6 TARGET AREA AT THE LAMPF BEAM STOP FACILITY

Figure 10. Aluminum Case Used to Protect Mirrors
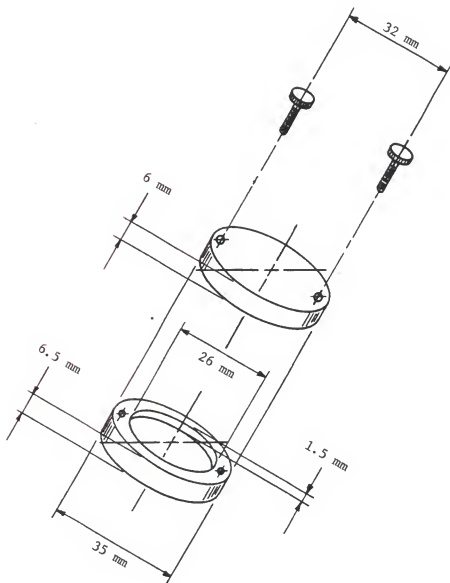During Neutron Irradiation.

Figure 11. Top View, A-6 Target Area, Showing the Proton Irradiation (A-C) and Neutron Irradiation (1-12) Boxes.
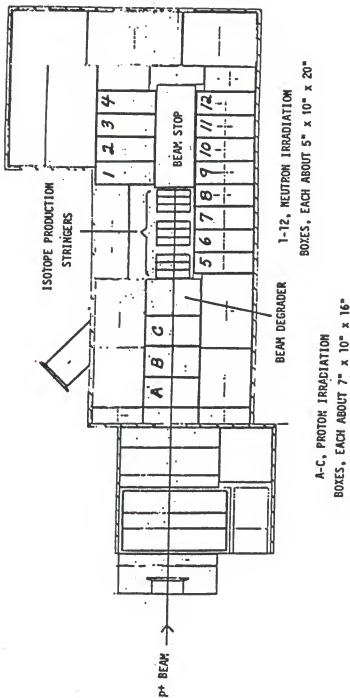
66
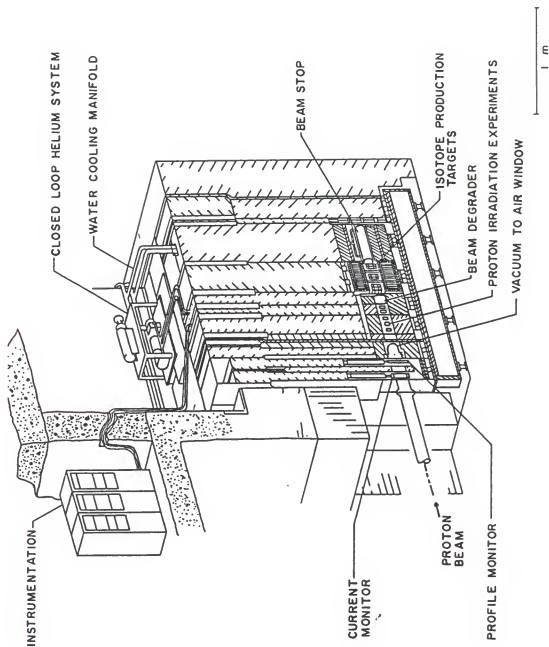
Figure 12. Layout of A-6 Target Area at LAMPF Beam Stop

CLOSED LOOP HELIUM SYSTEM

WATER COOLING MANIFOLD

BEAM STOP

ISOTOPE PRODUCTION TARGETS

BEAM DEGRADER

PROTON IRRADIATION EXPERIMENTS

VACUUM TO AIR WINDOW

1 m

INSTRUMENTATION

CURRENT MONITOR

PROTON BEAM

PROFILE MONITOR

Figure 13. Station A-6 Neutron Irradiation Area at LAMPF Beam Stop.

GAS, WATER, INSTRUMENTATION PASSAGE TO LABORATORY ABOVE

WATER COOLED SHIELDING

IRRADIATION VOLUME ~5x10x20″ 12 PLACES

3″ DIA., 9 DISKS EQUALLY SPACED

PROTON BEAM

150 mm

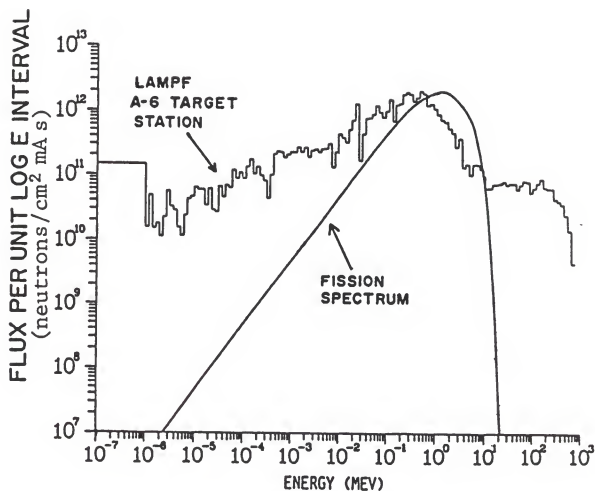NEUTRON PRODUCING TARGETS IN THE ISOTOPE PRODUCTION FACILITY

COPPER BEAM STOP

68
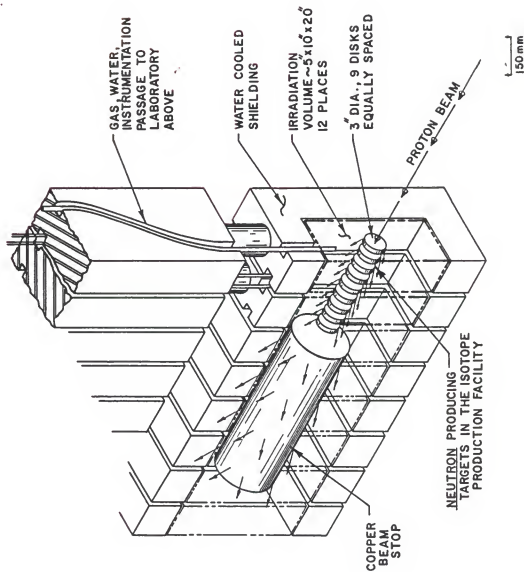
Figure 14. Neutron Energy Spectrum for A-6 Target Station at LAMPF Beam Stop.

13.4 APPENDIX D

GAMMA RAY IRRADIATION TEXT

REFLECTIVITY CURVES

Figure 15. Reflecitivity Curve for Iodine Laser Mirror #3.
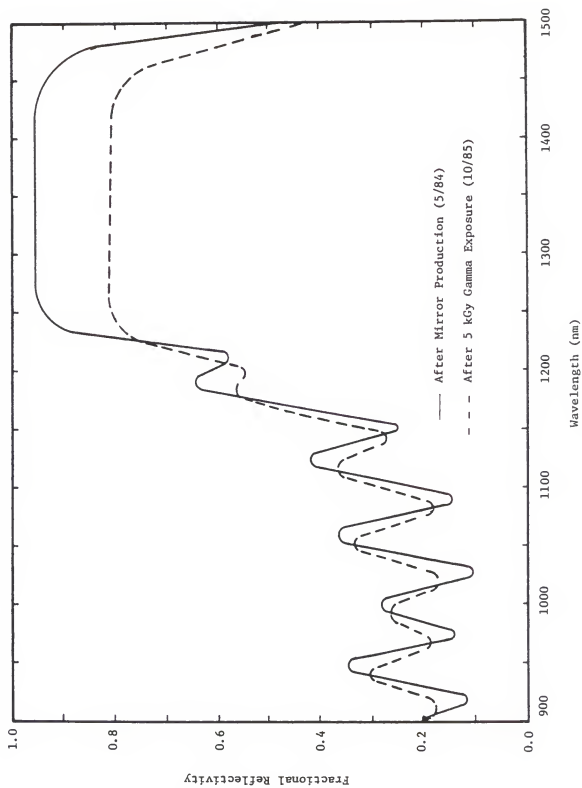
— After Mirror Production (5/84)
- - - After 5 kGy Gamma Exposure (10/85)

Wavelength (nm)

Fractional Reflecitivity

71

Figure 16. Reflectivity Curve for Iodine Laser Mirror #4.

After Mirror Production (5/84)
After 10 kGy Gamma Exposure (10/85)

Wavelength (nm)

Fractional Reflectivity
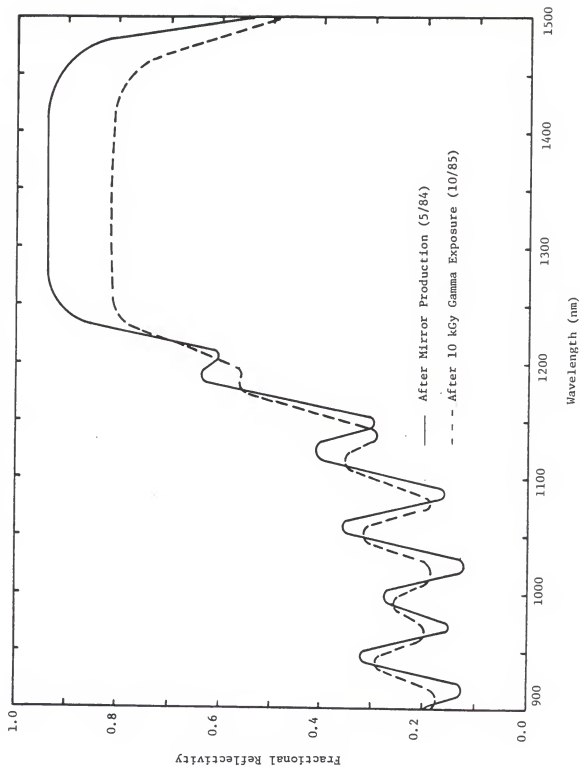
Figure 17. Reflectivity Curve for Iodine Laser Mirror #5.

After Mirror Production (5/84)

After 20 kGy Gamma Exposure (10/85)

Wavelength (nm)

Fractional Reflectivity

73
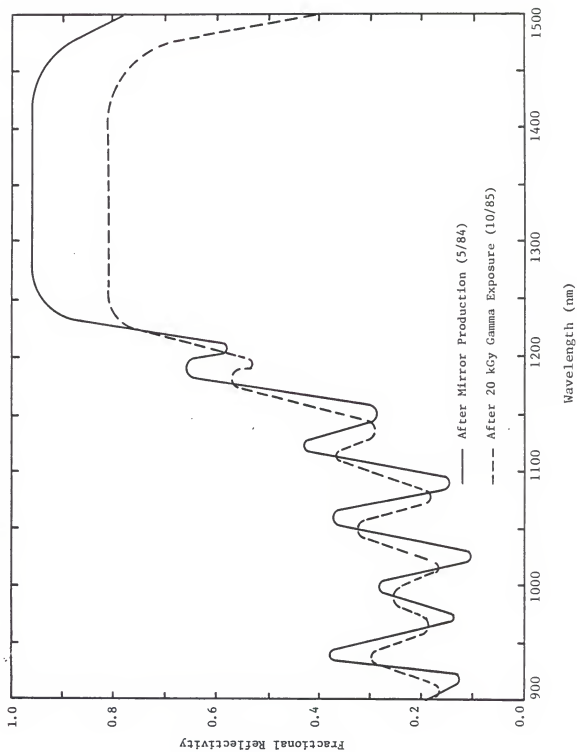
Figure 18. Reflectivity Curve for Iodine Laser Mirror #8.

— After Mirror Production (5/84)
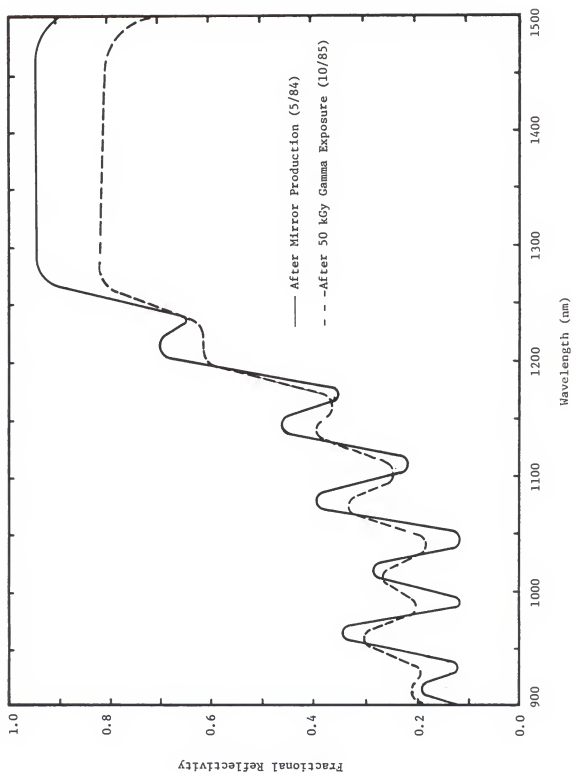- - - After 50 kGy Gamma Exposure (10/85)

Wavelength (nm)

Fractional Reflectivity

Figure 19. Reflectivity Curve for Iodine Laser Mirror #9.

75
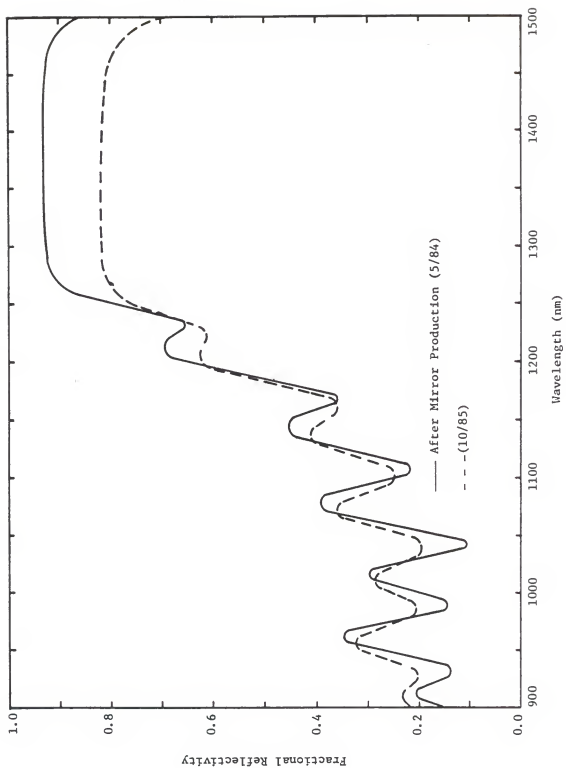
Figure 20. Reflectivity Curve for Iodine Laser Mirror #10.
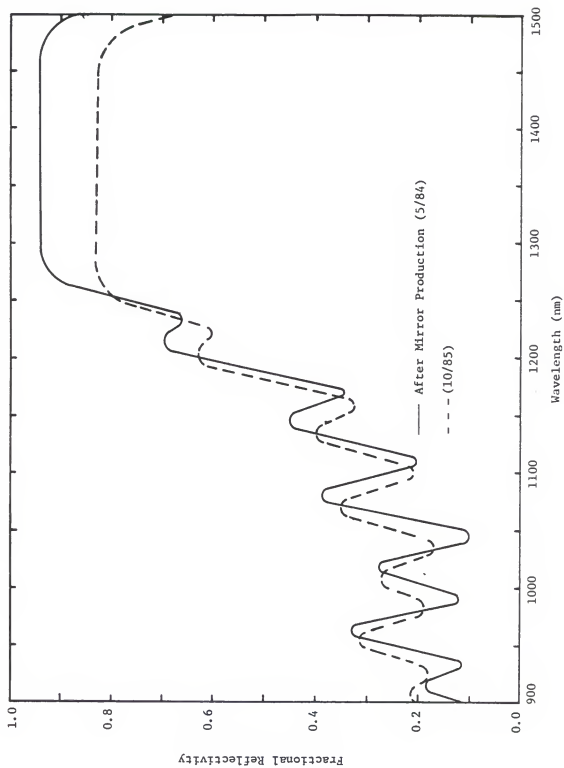
After Mirror Production (5/84) ———
(10/85) – – –

Wavelength (nm)

Fractional Reflectivity

76

THE EFFECTS OF RADIATION ON THE OPTICAL CHARACTERISTICS

OF (SiO$_2$ + ZrO$_2$ on Si Substrate) MIRRORS

by

MARK ANTHONY FERREL

B.S., Emporia State University, 1983
B.S., Kansas State University, 1984

————————————

AN ABSTRACT OF A MASTER'S THESIS

submitted in partial fulfillment of the
requirements for the degree

MASTER OF SCIENCE

Department of Nuclear Engineering

KANSAS STATE UNIVERSITY

Manhattan, Kansas

1986

ABSTRACT

Radiation induced absorption in optical components has recently become the concern of at least two projects, the Strategic Defense Initiative and Inertial Confinement Fusion. This is an unexplored area, and several projects have been undertaken to gather information about optical components' vulnerability to radiation. One such optical component tested was (SiO_2 + ZrO_2 on Si Substrate) iodine laser mirrors.

The following exponential was found to predict the probability of damage to mirrors (with 98% reflective at λ = 1.315 μm) at a given iodine laser (λ = 1.315 μm) fluence "F".

$$D = 1 - e^{(-8.60 \ \mu m^2/J) (F-0.275 \ MJ/m^2)} \pm 0.053$$

This predicts a 50% damage threshold of (0.355 $\pm$ .015) MJ/m^2. When mirror reflectivity is 83% (λ = 1.315 μm) the 50% damage threshold drops 20.6% to (0.282 $\pm$ .008) MJ/m^2.

A neutron fluence of 1.5×10^{22} neutrons/m^2 decreased the reflectivity of the mirrors by an average of 27.4% from 0.984 reflective (λ = 1.315 μm). Substantial damage was visible in the form of flaking of the SiO_2 and ZrO_2 dielectric coatings.

Gamma-ray doses up to 5.0 Mrad decreased the reflectivity by less than 3.5% at 1.315 μm. However, in the course of the gamma-ray tests it was discovered that over a period of approximately 1.3 years the reflectivity of non-irradiated control mirrors had dropped an average of 11.6% at 1.315 μm and the reflectivity spectrum had shifted toward the ultraviolet.

Test results demonstrate that iodine laser mirrors due to either manufacturing materials and/or techniques are not reliably radiation hardened for long-term use.